13th World Conference on Earthquake Engineering
Vancouver, B.C., Canada
August 1-6, 2004
Paper No. 312

SHEAR STRENGTH CAPACITY OF PRESTRESSED CONCRETE BEAM-COLUMN JOINT FOCUSING ON TENDON ANCHORAGE LOCATION

Wei YUE[1], Minehiro NISHIYAMA[2] and Fumio WATANABE[3]

SUMMARY

In order to estimate shear strength capacity and overall seismic behavior of prestressed beam-column joint assemblages, seven test units were constructed and tested under earthquake-simulating cyclic loads. The main experimental parameters were location of tendon anchorage, concrete compressive strength and prestressing steel content in the beam section. A reinforced concrete beam-column joint assemblage whose beam section has as large a moment capacity as the prestressed concrete test units was included in the test program. The test units failed in shear and tendon anchorage deteriorated in the joint core. Load carrying capacity, ultimate displacement, hysteretic energy, joint shear distortion were obtained and discussed. The joint shear strength of the test units were compared with those obtained by code specifications, such as the AIJ guidelines [1] and New Zealand concrete design code NZS3101. It should be noted that location of tendon anchorage had a great influence on shear capacity of the joint and load-displacement relation of the assemblages. The prestress on the joints was not so effective as the NZS3101 code specifies.

INTRODUCTION

New Zealand concrete design code, NZS3101: 1995 is innovative with respect to prestressed concrete because it specifies the effect of prestress on shear strength capacity of beam-column joints, and it includes other provisions which are not seen in current design codes in other countries. Especially it specifies that tendon anchorages should be placed outside the joint core. Architects generally want to have tendon anchorage inside the joint core, and structural engineers may have misgivings. However, it is not the provision that was proved by experimental results. In addition, the beneficial effect of prestress on shear strength of beam-column joint cores is still controversial.

Yue et al. [2] and Suzuki et al. [3] investigated the effect of location of prestressing tendon anchorage on beam-column joint behavior. The following conclusions are derived from their research works. The maximum load capacity of the specimens with inside anchorage was smaller than those with outside anchorage and the shear distortion was larger. The authors did not mention what kind of failure mode took

[1] PhD candidate, Dept. of Architecture Engineering, Kyoto University, Japan, rc.yue@archi-kyoto-u.ac.jp
[2] Associate Professor, Dept. of Urban and Environment Engineering, Kyoto University, Japan
[3] Professor, Dept. of Architecture Engineering, Kyoto University, Japan

place in their experimental programs, and joint shear strength was not quantitatively investigated. In this study failure modes as well as shear strength capacity and seismic performance of prestressed beam-column joints are examined in detail based on experimental results.

EXPERIMENTAL WORK

Outline of test specimens

Seven half-scale exterior beam-column assemblages were constructed and tested. The column was 250mm square section and the beam was 200mm in width and 300mm in depth. Six of the seven specimens had their beam prestressed, while the last one was an ordinary reinforced concrete unit. Details of the typical test unit are shown in Figure 1. The test parameters were: (1) the ratio λ defined as the ratio of the prestressing steel contribution to the beam flexural moment capacity (λ=0.49, 0.73 and 0.76), (2) location of prestressing tendon anchorage (0.75Dc and 0.5Dc measured from the beam-column interface, where Dc is the column whole depth), (3) concrete compressive strength (design concrete compressive strengths were 30 N/mm^2 and 50 N/mm^2), (4) prestressed or ordinary reinforced concrete beam. The test variables are summarized in Table 1. All specimens were designed to have almost the same flexural strength. To prevent concrete flexural crashing in the beam in the early stage of loading, lateral confining reinforcement was provided at the 50mm spacing in the potential plastic hinge region. Effective prestress of each test unit was about 60% of the nominal yield strength of the tendon as shown in Table 1. Material properties of the materials are summarized in Table 2.

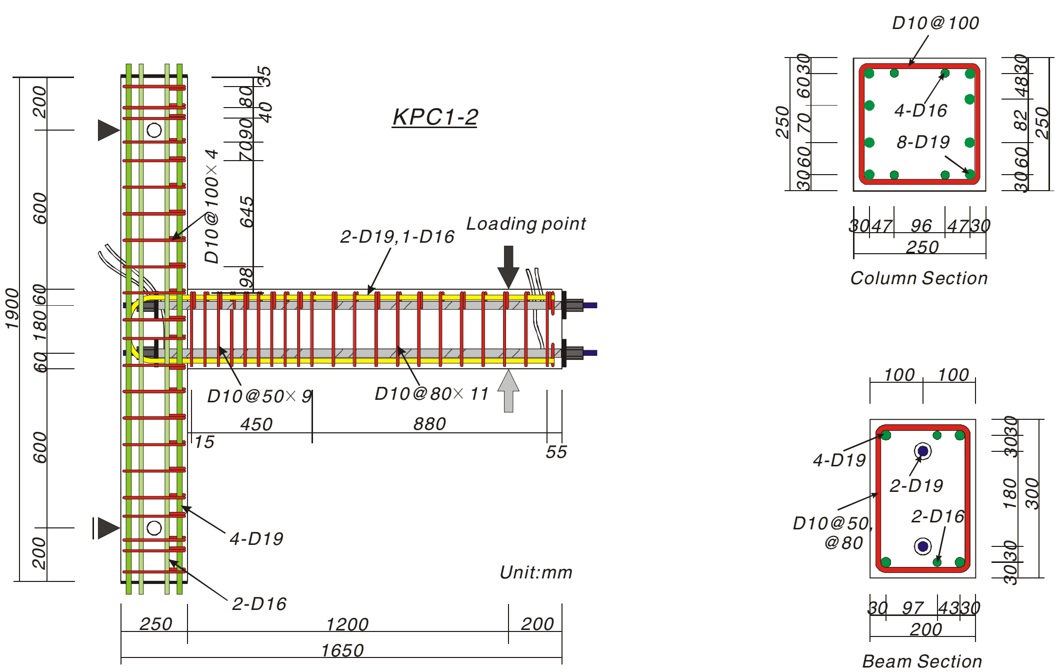

Figure 1: Reinforcement details of the test unit KPC1-2

Table 1: Specifications of Test units

Test unit	Anchorage location	λ *	Design concrete compressive strength f'_c [N/mm^2]	Effective prestressing force P_e [kN]	Prestress level P_e/bDf'_c
KPC1-1	Outside	0.49	30	323.6(0.61f_{py})	0.12
KPC1-2	Inside(0.5Dc)	0.49	30	314.4(0.59f_{py})	0.12
KPC2-1	Outside	0.73	30	555.6(0.59f_{py})	0.27
KPC2-2	Inside(0.75Dc)	0.73	30	556.2(0.59f_{py})	0.27
KPC2-3	Inside(0.5Dc)	0.73	30	538.2(0.57f_{py})	0.26
KPC3	Inside(0.5Dc)	0.76	50	599.4(0.64f_{py})	0.16
KRC	-	-	30	-	-

f_{py}: yield strength of prestressing steel, b: beam width, D: beam depth.
* Based on the material strengths in Table 2 and ACI concrete stress block.

Table 2: Material mechanical properties

(a) Steel

Bar		Yield strength [N/mm^2]	Young's modulus [10^{5}N/mm^2]	Tensile strength [N/mm^2]
Deformed prestressing steel bar	D19	1064	2.01	1176
	D25	1026		1146
Mild steel	D10	307	1.76	437
	D16	375	1.85	533
	D19	387	1.83	570
	D25	417	1.88	614

(b) Concrete

Tste unit	Compressive strength f'_c [N/mm^2]	Tensile strength f_t [N/mm^2]	Young's modulus E_c 10^{4}N/mm^2]
KPC1-1, KPC1-2	45.5	3.27	3.30
KPC2-1, KPC2-2, KPC2-3	34.6	2.51	2.82
KRC	45.5	3.27	3.30
KPC3	64.3	-	3.43

Loading setup and Measurements

The specimen was rotated by 90 degrees and set in the loading rig as schematically shown in Figure 2. A horizontal load was applied at the end of the beam representing shear induced by seismic loading. The ends of the column were held on the same horizontal line between the pin and roller supports during the test and the applied beam load induced reactive shear force in the column. Loading cycles imposed were consisted of two full cycles at each of the following beam rotation angles: 0.5%, 1.0%, 2%, 3%, 4%, 5%, 7.5%.

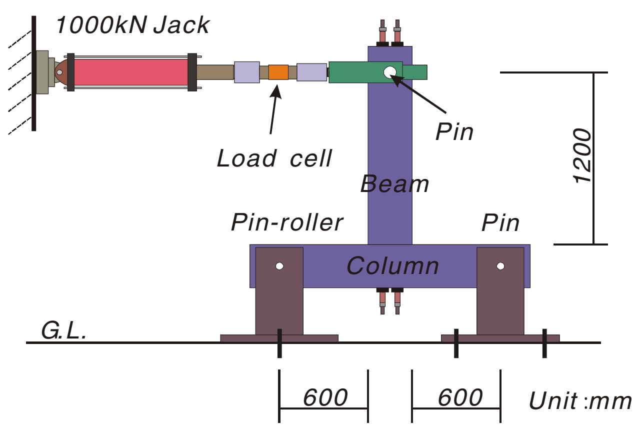

Figure 2: Loading setup

The measured items were applied load and deflection at the beam end, deformation of the beam-column joint panel and potential plastic hinge regions of the beam and column, strains of the prestressing tendons, beam longitudinal reinforcements and transverse reinforcements.

EXPERIMENTAL RESULTS AND DISCUSSIONS

Shear cracking strength of beam-column joint panel

Table 3 summarizes the joint shear force when shear crack was first observed in the beam-column joint panel. Joint shear crack strength V_{jc} was calculated based on principal tensile stress using Eq. 1. It is assumed that shear crack occurred when the principal tensile stress exceeded the concrete tensile strength.

$$V_{jc} = b_j D_c \sqrt{\sigma_t^2 + \frac{P_e}{bD}\sigma_t}$$

Eq. 1

where b_j: joint effective width, $b_j=(b+b_c)/2$, b is the beam width, b_c is the column width. D_c: column whole depth, σ_t: concrete tensile strength ($\sigma_t = 0.626\sqrt{f_c^{'}}$ according to the reference [4], $f_c^{'}$ is the concrete compressive strength.), P_e: effective prestressing force, D: beam whole depth.

V_{jc} was transferred to the beam shear force $V_{cr,cal}$ using Eq. 2 and compared with the experimental results listed in Table 3. The shear cracking loads of the test units with inside tendon anchorage was smaller than those with outside anchorage.

$$V_{cr.cal} = V_{jc} \frac{2 j_b}{L - D_c - \frac{L}{H} j_b}$$

Eq. 2

where, j_b: internal lever arm of the beam section (=7/8d, d is effective depth), H: story height,. L: beam span (twice the distance from the loading point to the center of the joint core).

Table 3: Joint shear cracking load

Unit	Cracking load V_{cr} [kN]	Calculated cracking load $V_{cr.cal}$ [kN]	$V_{cr}/V_{cr.cal}$
KPC1-1	56.4	70.9(61.8)	0.80(0.91)
KPC1-2	42.2	70.5(60.1)	0.60(0.70)
KPC2-1	52.2	71.9(56.8)	0.73(0.91)
KPC2-2	45.3	71.9(55.6)	0.63(0.92)
KPC2-3	32.3	71.3(51.7)	0.45(0.62)
KPC3	36.8	92.4(73.8)	0.40(0.50)
KRC	36.7	56.6(56.6)	0.65(0.65)

The axial compressive stress in the joint due to the effective prestressing force P_e of the Eq. 1 was calculated as P_e/bD based on the beam section. However, the actual axial compressive stress induced in the joint should be smaller than that. Then, the axial compressive stress induced in the joint by the beam prestress was estimated using measured longitudinal strains of the shear reinforcement in the joint at the introduction of prestress and is shown in Table 4. The shear reinforcement strains are assumed to represent the average concrete strain in the joint. The closer the tendon anchorage was located to the joint center, the smaller the shear reinforcement strains were, which indicates that the effective prestressing force in the beam was not fully transferred into the joint. The axial concrete compressive stresses in the joint predicted by the strain readings of the shear reinforcement in the joint ranged from 34% to 9% of the average prestress in the beam section. Shear cracking loads considering $\sigma_{cj} / \sigma_{cb}$ ratio shown in the last column of Table 4 are listed in the parentheses in Table 3. These are closer to the experimental results.

Table 4: Shear reinforcement strain measured in the joint at the introduction of prestress

Unit	Average compressive strain of shear reinforcement in joint ε_{sj} [10^{-6}]	$\sigma_{cj}=E_c\ \varepsilon_{sj}$ [N/mm^2]	Average prestressing stress of beam section σ_{cb} [N/mm^2]	σ_{cj}/σ_{cb}
KPC1-1	64	2.11	6.21	0.34
KPC1-2	44	1.45	6.41	0.23
KPC2-1	116	3.27	11.4	0.29
KPC2-2	94	2.65	11.2	0.24
KPC2-3	35	0.99	10.8	0.09
KPC3	77	2.64	11.5	0.23

Beam end load-beam rotation angle relations and maximum load capacity

Applied load at the beam end plotted against beam rotation angle is illustrated in Figure 3. Hysteresis loops of all the test units are pinched with small energy dissipation. Effect of tendon anchorage location and prestressing force were not clearly observed. The hysteresis loops of the reinforced concrete unit KRC were narrower than the corresponding prestressed concrete units KPC1-1 and KPC1-2. Before the maximum load of the beam end was reached, beam ordinary longitudinal reinforcements yielded. In KPC1-1 with the anchorage outside the joint core, just before the maximum load of the beam end reached, the prestressing steel yielded. In KPC3 with the highest strength concrete, after the peak load was reached prestressing steel yielded. The prestressing steel in the other units did not yield.

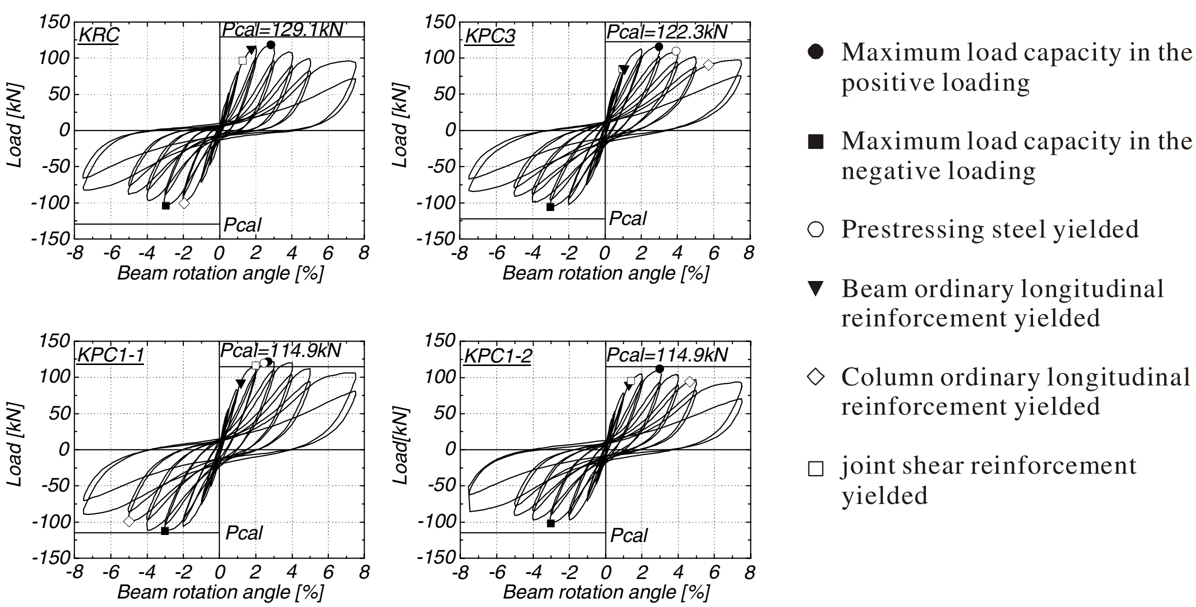

Figure 3: Load-beam rotation angle (continued)

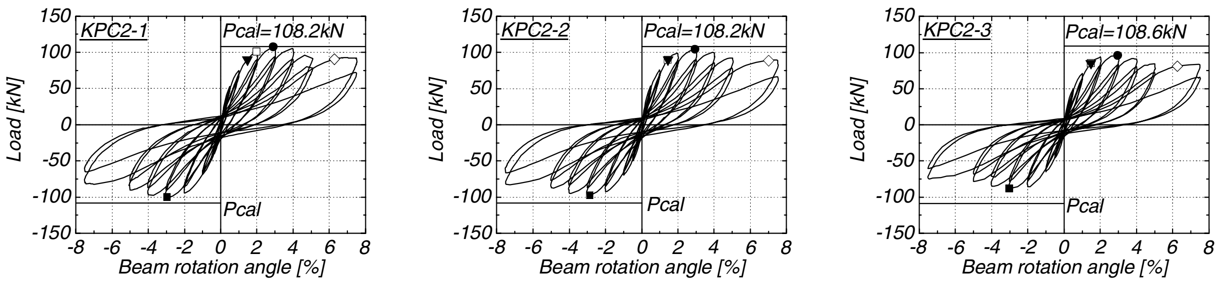

Figure 3: Load-beam rotation angle

Table 5 shows the maximum experimental loads at the beam end $V_{b\ max}$. P_{cal} is the load corresponding to the flexural capacity of the beam section calculated by the ACI318 method and the measured material strengths. Only KPC1-1 with the anchorage outside the joint core reached the calculated flexural capacity P_{cal}. For test units KPC1-1 and KPC2-1 with the outside anchorage, the maximum load of the beam end (average of the positive and negative values), were larger than test units KPC1-2 and KPC2-3 with the inside anchorage by 9% and 13%, respectively.

Table 5: Maximum load capacities obtained experimentally and calculated by ACI concrete stress block

Unit	Loading direction *	Beam rotation angle [%]	Maximum load capacity V_{bmax} [kN]	Beam flexural capacity P_{cal} [kN]	V_{bmax}/P_{cal}
KPC1-1	+	2.7	121.5	114.9	1.06
	-	3.0	112.5		0.98
KPC1-2	+	3.0	111.6	114.9	0.97
	-	3.0	102.2		0.89
KPC2-1	+	3.0	107.3	108.2	0.99
	-	3.0	100.7		0.93
KPC2-2	+	3.0	104.1	108.2	0.96
	-	2.9	97.8		0.90
KPC2-3	+	3.0	95.4	108.6	0.88
	-	3.0	88.1		0.81
KPC3	+	3.0	115.3	122.3	0.94
	-	3.0	106		0.87
KRC	+	2.9	118.1	129.1	0.92
	-	3.0	104.5		0.81

* +: positive cycles, -: negative cycles

Joint shear deformation

Four main components are considered dominant for the total beam end displacement. These components are:

D_j: shear distortion of the beam-column joint core.

D_b: flexural deformation in the beam potential plastic hinge region.

D_c: flexural deformation in the column potential plastic hinge region.

D_{b1}: flexural deformation in the beam outside the potential plastic hinge region (calculated based on elastic stiffness).

Contributions of these components to the beam end displacement are shown in Figure 4. From the figure it was observed that with the beam rotation angle increasing the ratio of the joint shear deformation increased. The following observations are derived by comparing the components to the joint shear distortion of all units at the final loading cycle. KPC1-2 with the anchorage inside the joint core was 28%

larger than KPC1-1 with the outside anchorage. KPC2-3 was 17% and 41% larger than KPC2-2 and KPC2-1, respectively. It can be concluded that when the tendon anchorage is placed outside the joint, the shear deformation decreased.

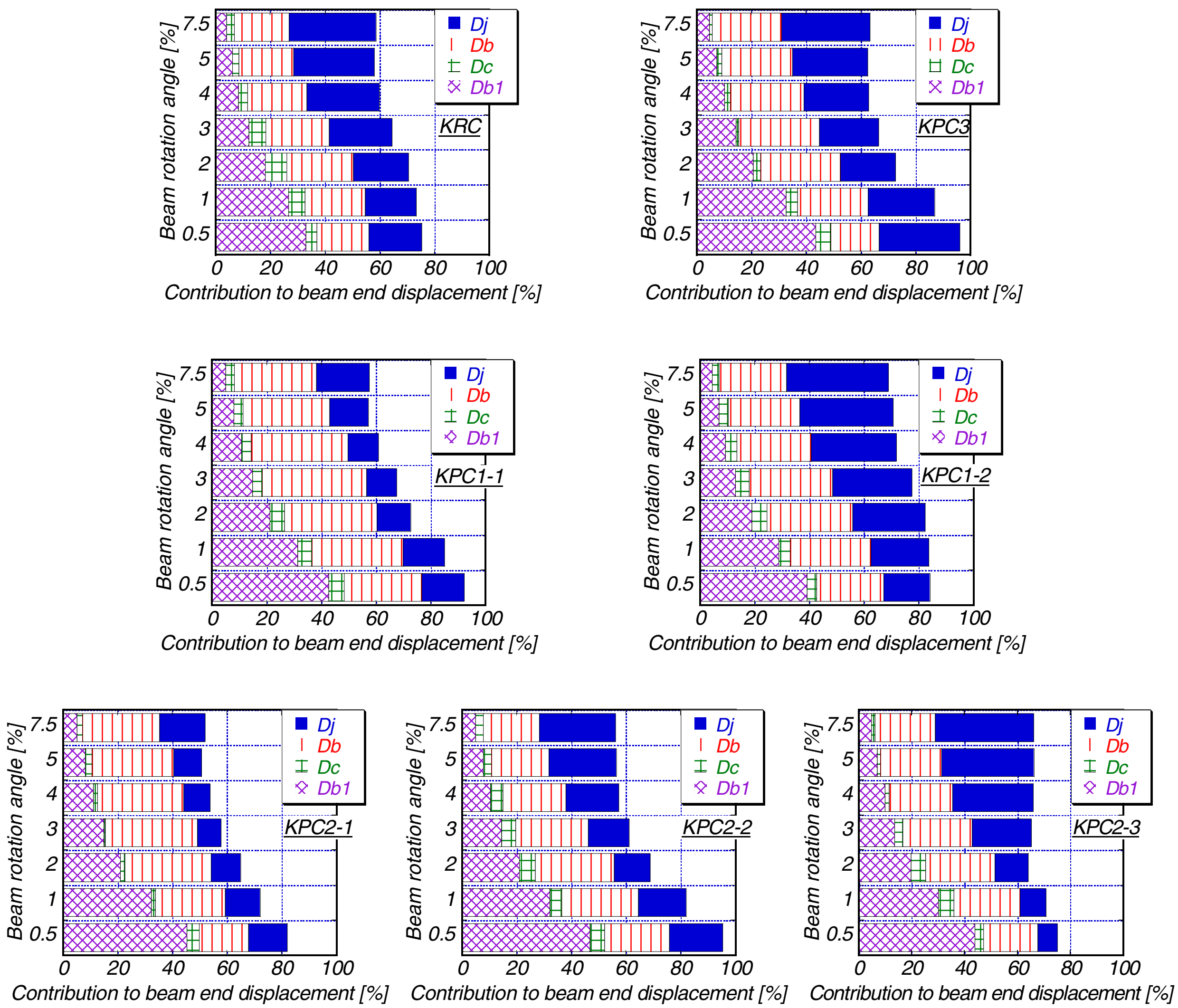

Figure 4: Contribution of each deformation component to the overall beam deflection

Failure modes

Crack pattern of each specimen at the end of loading is shown in Figure 5. The drawn area in the figure includes only the joint panel and the potential plastic hinge region of columns and beam. As displacement amplitude increased, cracks in the joint panel extended, and at the final stage of loading concrete crashing in the joint panel was observed for all test units.

In case of inside joint anchorage, damage can be considered either due to joint shear failure or to anchorage deterioration of prestressing steel bars. To investigate a dominant failure mode of each test unit the following points were considered:

1) Deformation where ordinary longitudinal reinforcement reached its yield strain,
2) Deformation where prestressing steel reached its yield strain,

3) Comparison between the load at the beam end and the joint shear force input calculated based on the equilibrium of forces in the joint core,
4) Observed damage,
5) Joint shear distortion angle, and
6) Contribution of joint shear deformation to the total displacement.

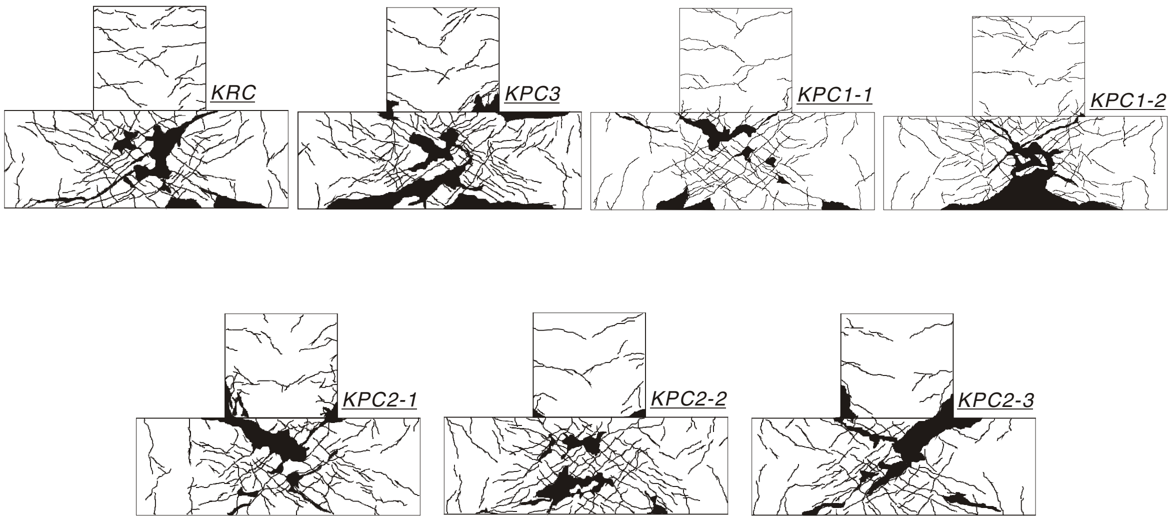

Figure 5: Crack pattern after testing

Joint shear failure was observed for units KPC3, KRC and KPC1-1 after yielding of beam longitudinal reinforcements. Units KPC3 and KRC reached their maximum loads at the beam rotation angle of 3%, after that load capacity reduced as shown in Figure 3. These two units had their ordinary longitudinal reinforcement and prestressing steel in the beams yielded, indicating that the beam flexural strength was reached. In unit KPC1-1, after the prestressing steel yielded, the maximum load was attained at the beam rotation angle of 2.7%, which corresponded to the beam flexural strength. However, in units KPC3, KRC and KPC1-1, components of joint shear distortion contribution to the total displacement and shear strain in the joint core increased as loading progressed as shown in Figure 4 and in Figure 6, respectively.

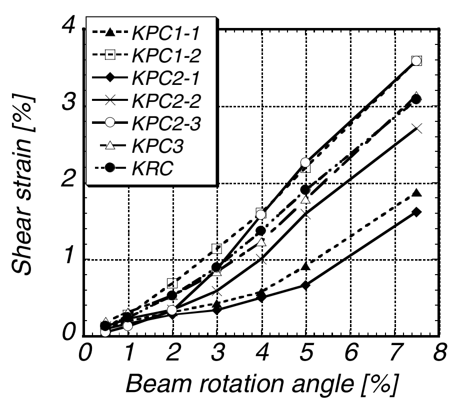

Figure 6: shear strain of joint

Unit KPC2-1 and KPC2-2 failed in shear in the joint. In the two test units ordinary longitudinal reinforcements yielded, but prestressing steel did not yield. Hence, the beam flexural strength was not reached. Figure 7 shows that the joint shear input reached its maximum at the beam rotation angle of 2% however, in Table 5 the maximum load for the two test units was reached at the beam rotation angle of approximately 3%, indicating that load capacity decayed due to joint shear failure.

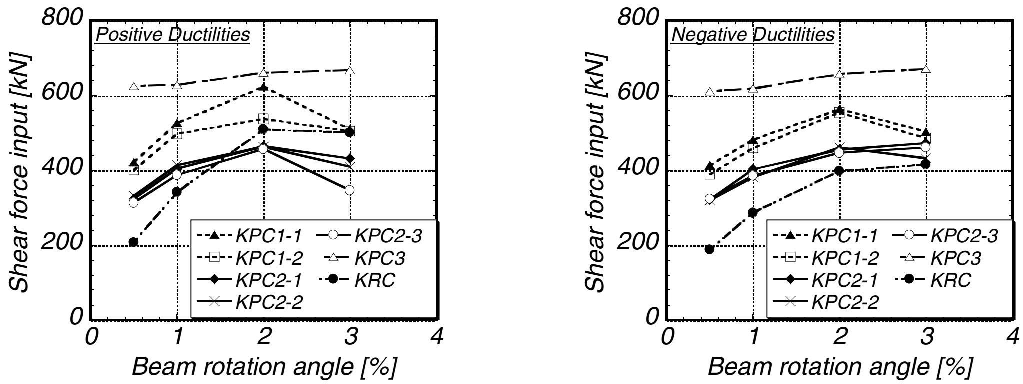

Figure 7: joint shear input

The anchorage deterioration of prestressing steel bar occurred in KPC1-2 and KPC2-3, with inside anchorage. As shown in Figure 6, joint shear strains in these two test units were the largest among all the test units. Prestressing steel tensile force increments for KPC1-2 were smaller than KPC1-1 and also for KPC2-3 while compared to KPC2-1 and KPC2-2, as shown in Figure 8. This indicated that the prestressing forces did not fully develop, the tendon anchorage deteriorated in these two test units.

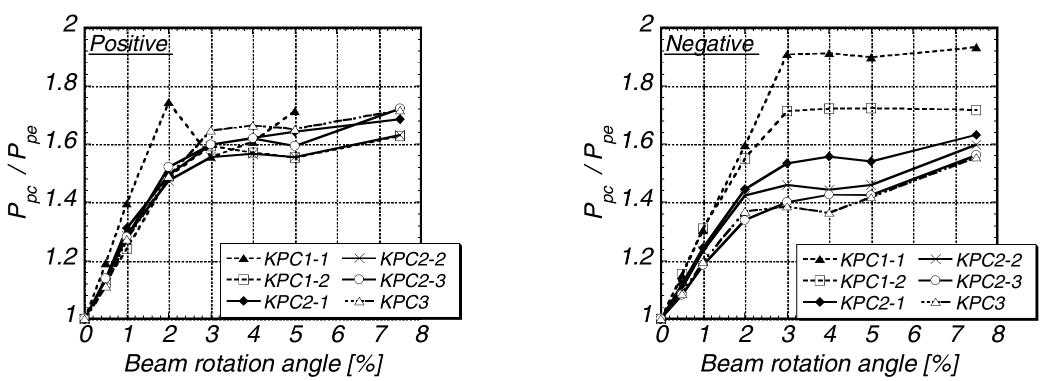

Figure 8: Envelope curves of the tensile forces in the prestressing steel bars

Ultimate input shear force and shear strength of joint

Experimental input joint shear force was computed from equilibrium of column shear force and axial forces in reinforcements and prestressing steel bars as shown in Figure 9. Forces in the reinforcements and prestressing steel bars were estimated using the measured strains and the stress-strain models in the references [5][6].

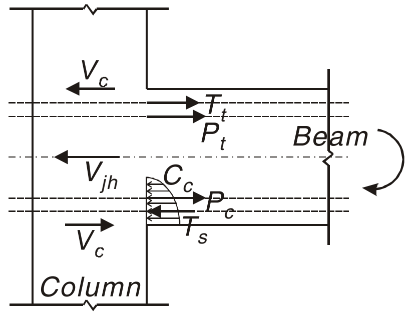

Figure 9: Input shear force of joint

The ultimate joint shear input and the shear strength of the test units are summarized in Table 6. $V_{j\text{-NZS}}$ was calculated based on the New Zealand concrete design code NZS3101, specifying that the nominal horizontal joint shear stress shall not exceed $0.2f_c^{'}$. $V_{j\text{-AIJ}}$ was calculated from Eq. 3 proposed by the AIJ guideline [1].

Table 6: Ultimate input shear force and shear strength of joint

Test unit	$expV_j$ [kN]		$V_{j\text{-NZS}}$ [kN]	$V_{j\text{-AIJ}}$ [kN]	$expV_j$ / $V_{j\text{-NZS}}$		$expV_j$ / $V_{j\text{-AIJ}}$	
	+	-			+	-	+	-
KPC1-1	590.9	563.5	511.8	450.5	1.16	1.10	1.31	1.25
KPC1-2	537.7	554.9			1.05	1.08	1.19	1.23
KPC2-1	464.8	473.4	389.3	370.1	1.19	1.22	1.26	1.28
KPC2-2	463.3	461.4			1.19	1.19	1.25	1.25
KPC2-3	457.1	446.8			1.17	1.15	1.24	1.21
KPC3	667.9	671.1	723.4	577.5	0.92	0.93	1.16	1.16
KRC	509.7	416.1	511.8	450.5	0.99	0.81	1.13	0.92

* +: positive cycles, -: negative cycles

$$V_{j-AIJ} = 0.587\sigma_B^{0.718} b_j D_j$$

Eq. 3

where, σ_B: concrete compressive strength, b_j: joint effective width, D_j: anchorage length of beam longitudinal reinforcement.

Ratios of the ultimate input joint shear force to joint shear strength calculated according to NZS3101 and the AIJ guidelines are also shown in Table 6. Except for units KPC3 and KRC, the ultimate input joint shear forces were 5~22% larger than the joint shear strength of NZS3101, and except for KRC at the negative cycles the ratios ranged from 13% to 31% while using the AIJ guideline. The maximum input joint shear forces of KPC3 and KRC were smaller than the joint shear strengths by NZS3101. This indicates that, the AIJ guideline underestimates the joint shear strength.

Comparison of the ultimate joint shear force of each unit with different anchorage location is given in Table 6. The ultimate joint shear strengths of the units with the outside anchorage are larger than the units with the inside anchorage. KPC3 with the highest strength concrete had the biggest ultimate input shear force, which proved that the joint shear strength was dominated by concrete compressive strength.

CONCLUSIONS

1) The joint shear cracking load was small in the test units with inside anchorage, because the full effective prestressing force in the beam was not transferred into the joint.
2) The maximum load capacities for the units with the inside anchorage 9% to 13% smaller than those having their anchorage outside the joint core.
3) The joint shear deformation was small in the test units with the outside anchorage. The ultimate input joint shear force in the units with the outside anchorage was larger than the units with the inside anchorage.
4) Comparing the joint shear strength obtained by NZS3101 and the AIJ design guideline with the test results, it was found that the AIJ guideline underestimated the joint shear strength more than NZS3101 code.
5) Damage to the beam-column joint assemblages and the decay of the maximum capacities of the test units were not due only to joint shear failure, but to the anchorage deterioration of prestressing steel bar also.

ACKNOWLEDGEMENT

The work reported in this paper as a part of cooperative research project was sponsored by the committee of prestressed concrete beam-column joint (Chairman: Professor F. watanabe, Kyoto University), and organized by Japan Prestressed Concrete Engineering Association. The authors wish to express their gratitude to them. And thanks are extended to Neturen, Co., Ltd. for providing prestressing steel.

REFERENCES

[1] Architectural Institute of Japan: Design Guidelines for Earthquake Resistant Reinforced Concrete Buildings Based on Inelastic Displacement Concept, 1999.

[2] Yue W., Hamada Y. and Nishiyama M., "Influences of anchorage position of prestressing steel on joint strength of beam-column joint subassemblage", proceeding of AIJ Annual Meeting 2001, pp. 927-930 (in Japanese).

[3] Suzuki N. et al., "Experimental Study on Ultimate Strength of Exterior Beam-Column Joint in Prestressed Concrete Frame" proceeding of AIJ Annual Meeting 2003, pp.1009-1014 (in Japanese).

[4] Architectural Institute of Japan: State-of-the-Art Report on High-Strength Concrete, 1991.

[5] F. J. Vecchio, "Towards Cyclic Load Modeling of Reinforced Concrete", ACI Structural Journal, V. 96, No. 2, March-April 1999.

[6] F. A. Zahn, "The Ductility of Bridges", Ph. D. Thesis, University of Canterbury, 1985.